

Recent ORNL measurements of chemical sputtering of ATJ graphite by slow atomic and molecular D ions

F W Meyer, L I Vergara and H F Krause

Physics Division, Oak Ridge National Laboratory, Oak Ridge, TN 37831 6372, USA

E-mail: meyerfw@ornl.gov

Received 14 June 2005

Accepted for publication 17 November 2005

Published xx February 2006

Online at stacks.iop.org/PhysScr/73/1

Abstract

We describe here an ORNL Physics Division research activity whose focus is the investigation of chemical sputtering of graphite by atomic and molecular D ions at very low energies that have so far been unexplored. Our initial experimental approach is based on the use of a quadrupole mass spectrometer (QMS) which samples the partial pressure of selected mass species produced in a scattering chamber when the incident ion beam strikes a graphite sample. While most of the ORNL results obtained to date are for D_2^+ ions incident on ATJ graphite, preliminary results are shown for D^+ projectiles incident at energies down to 10 eV D^{-1} , and for D_3^+ ions incident at 10 and 4.5 eV D^{-1} . The possibility of obtaining complementary information using a time-of-flight approach is discussed as well.

PACS numbers: 34.50.Dy, 52.20.Hv, 79.20.–m, 79.20.Rf

1. Introduction

As has been discussed in greater detail in other workshop contributions [1], there is a significant technological interest in using graphite as a plasma-facing component on present and future fusion devices, and in using different types of graphite or carbon fibre composites (CFCs), together with tungsten, beryllium or other refractory metals, in the ITER divertor. Motivated in part by this interest, an experimental research programme was recently started at the ORNL Multicharged Ion Research Facility (MIRF) [2] to investigate chemical sputtering of graphite surfaces in the limit of very low impact energies (i.e. below 10 eV D^{-1}), where there is currently no available experimental data. In addition to the exploration of very low impact energies, this research will focus on comparisons of atomic and molecular ion impact, to better determine the range where atomic and molecular species at the same velocity behave in an equivalent manner with respect to the chemical sputtering yields. We also discuss the possibility of initiating chemical sputtering measurements using a time-of-flight (TOF) approach to detect product radicals and greatly reduce or eliminate the need for ‘wall corrections’ presently needed to deduce the chemical sputtering yield.

To date, measurements at ORNL have focused on ATJ graphite, with the goal of comparing chemical sputtering

characteristics of virgin tiles and tiles recently removed from the DIII-D machine after 8 years of exposure to plasma shots. Measurements on ATJ graphite have been previously reported by the University of Toronto group [3, 4] using slow D_2^+ and D_3^+ projectiles at energies down to 15 eV D^{-1} .

Laboratory chemical sputtering studies by low energy ($< 200 \text{ eV}$) H/D ion impact have been previously reported by Mech *et al* [5, 6], Davis *et al* [7], Balden and Roth [8] and Yamada [9] for pyrolytic graphite. Studies on hydrogenated thin films (a-C:H) [10, 11] or pyrolytic graphite [7, 12] exposed to thermal hydrogen have been reported as well.

2. Experiment

All ORNL measurements to date were performed in a floating potential ultra-high vacuum chamber with base pressures in the 10^{-8} Pa range, shown schematically in figure 1, into which decelerated ion beams from an ECR ion source were directed, as previously described [13]. A sensitive quadrupole mass spectrometer (QMS) [14] was installed in place of the electrostatic spherical sector spectrometer shown in figure 1. A grounded baffle between the front end of the QMS and the target sample prevents field penetration from the QMS ionizer section into the region immediately in front of the

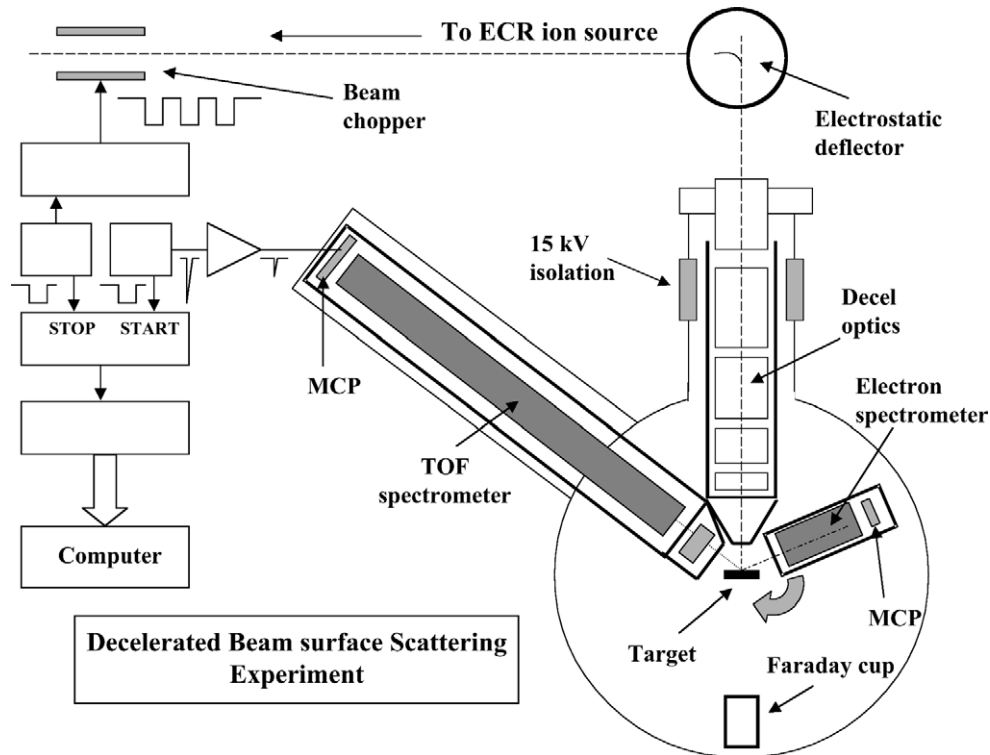


Figure 1. Schematic diagram of the decelerated beam surface scattering apparatus.

sample where the low-energy ion beam strikes the graphite target. This baffle also blocks the line-of-sight path between the sample and the analyser, along which scattered projectiles at higher beam energies could enter and cause unwanted backgrounds in the measured mass spectra. The chamber also contains a TOF analyser previously used for binary-collision backscattering studies [15].

A target fabricated from ATJ graphite (UCAR Carbon Co), the same material presently employed on the DIII-D device at General Atomics, was used for all our measurements. Prior to mounting, the target was pre-annealed for at least 4 h at a temperature of 1300 K in a vacuum furnace. The target temperature, controlled by electron-beam-heating from the rear, is monitored from the front using a calibrated infrared (IR) thermal monitor. Annealing at temperatures in excess of 1500 K was performed for about 45 s between measurements in order to reinitialize the H/D inventory in the graphite sample. The sample is located 15 mm downstream from the final aperture of the electrostatic deceleration system. For all our measurements to date, the mass selected projectile beam impacted the sample at normal incidence. As illustrated in figure 2(a), the incident ion beam spatial profile is approximately Gaussian with a width in the range 1–2 mm (FWHM) for the 30–250 eV D⁻¹ energy range, and about 5 mm for a 10 and 15 eV D⁻¹ ion beam; profiles are determined by a wire scanner that can be inserted in the plane of the target sample. Using the beam currents intercepted by the sample and the beam profile measurements, typical beam fluxes of $2\text{--}8 \times 10^{15}$ D cm⁻² s⁻¹ are inferred for the 30–250 eV D⁻¹ energy range. Fluxes in excess of 1×10^{14} D cm⁻² s⁻¹ are obtained for energies as low as 10 eV D⁻¹. As shown in figure 2(b), the energy spread of the decelerated beams is less than 10% down to a final energy of 10 eV and the spread is typically below 20% at yet

lower energies, as measured using the electrostatic spherical sector spectrometer mentioned earlier. Typical vacuum during the measurements (i.e. with decelerated beam in the UHV chamber) is in the mid 10^{-7} Pa range.

The present experimental approach uses a sensitive QMS which monitors the partial pressure of selected mass species in the scattering chamber throughout the 1–60 amu range. A Macintosh-based data acquisition system is used to measure mass distributions at fixed intervals in time, or alternatively, to follow the intensity of selected mass peaks versus beam exposure time. The evolution of peak intensities is measured versus accumulated beam dose until saturation occurs. It is crucial to the experimental approach that all contributions to the chamber pressure other than those related to the incident beam be kept constant during the irradiation runs. This allows the evolution of chemical sputtering products to be determined by taking differences between a pre-irradiation mass spectrum and one acquired during irradiation at progressively larger accumulated D target doses.

The incident ion intensity is determined from a direct current reading on the target sample after appropriate correction for secondary electron emission is made. This correction was based on *in situ* measurements for a few selected incident species and energies, and on the scalings with projectile energy and mass reported in [16].

The procedure used to deduce the partial chemical sputtering yields is described in [14, 17]. It involves selection of an analysis mass for each species of interest (in the present case CD₄ and C₂D₂), determining and correcting for the possible interferences due to cracking of heavier hydrocarbons, and placing the sputtering yields on an absolute scale using calibrated leaks [18]. In addition, the apparent yields must, in general, be corrected for wall

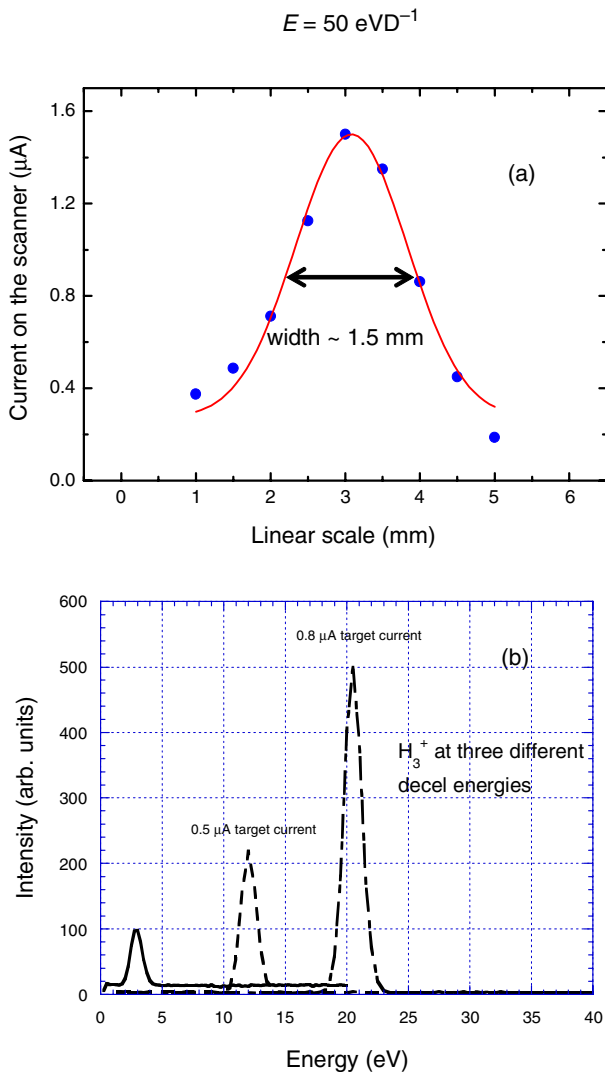


Figure 2. Typical (a) spatial and (b) energy characteristics of the decelerated beams. The spatial profile corresponds to a D_2^+ beam at 100 eV ; the energy spectra were measured earlier using H_3^+ projectiles; note that the energy scale refers to total kinetic energy, not eV H .

contributions, which can arise when the fraction of the incident deuterium beam reflected or re-emitted from the graphite target combines with hydrocarbon precursors on the interior vacuum chamber walls to form the sputtering products of interest. Such wall contributions are estimated from the initial steep rise observed in the chemical sputtering signal immediately after initiation of beam dosing, when the hydrogen concentration in the graphite is still too low to directly produce appreciable chemical sputtering products there. The effect of the wall contribution is illustrated in figure 3 for two different incident beam energies.

3. Sample results

Figure 4 summarizes our yields for the production of CD_4 and C_2D_2 at ATJ graphite temperatures of 300 and 800 K , the latter being close to the accepted maxima of the respective sputtering yields. Our results obtained using incident D_2^+ ions are indicated by circles and triangles. The bold dashed line indicates the room temperature trend for methane production

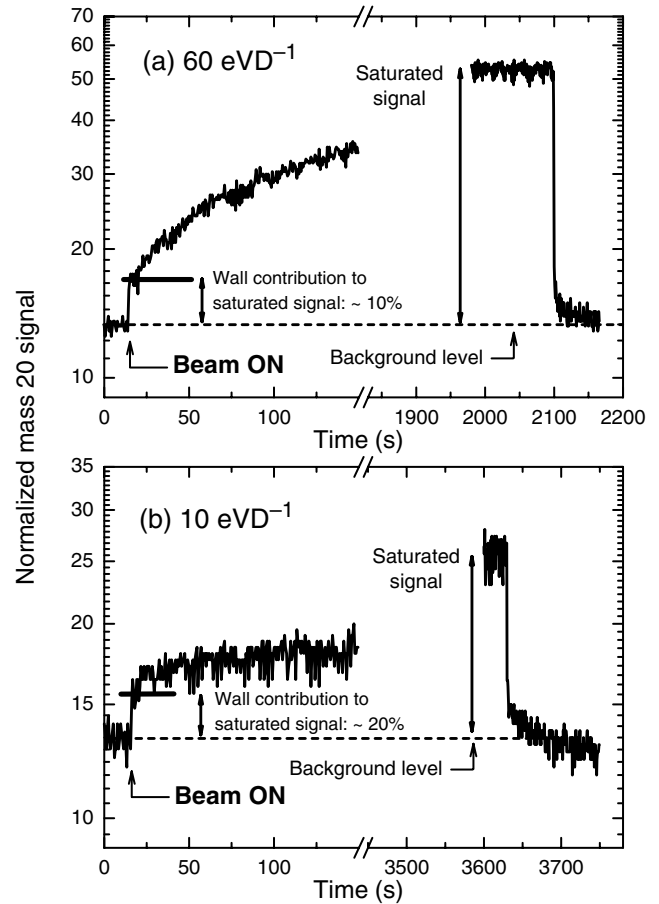


Figure 3. Time evolution of the CD_4 signal with incident (a) 60 eVD^{-1} D_2^+ and (b) 10 eVD^{-1} beam exposure, normalized to the incident beam current, illustrating the wall contribution effect when the beam is first turned on. Note return of the signal to background level when the beam is switched off after reaching saturation in the normalized CD_4 signal.

produced by D^+ incident ions. Also shown are recent results obtained by Wright *et al* [3], and, for comparison, chemical erosion yields for the same two hydrocarbons involving pyrolytic graphite and incident thermal H atoms (produced by thermal dissociation at $\sim 2500\text{ K}$), obtained by Davis *et al* [7]. Regarding the latter results, it is noted that the solid squares are chemical erosion yields obtained at a 500 K sample temperature, not room temperature; the yields denoted by open squares were obtained at a 800 K sample temperature.

As can be seen from the figure, the results for incident D^+ ions fall systematically below those for incident D_2^+ at energies below about 60 eVD^{-1} , reaching almost a factor of two difference at the lowest investigated energy of 10 eVD^{-1} . In view of the extensive use by other groups of D_3^+ projectiles to investigate chemical sputtering at the lowest reported incident energies, we have also begun measurements for the triatomic hydrogenic projectile ion. Figure 5 shows an acquired mass spectrum obtained at the lowest energy reached to date, 4.5 eVD^{-1} . In addition, a preliminary CD_4 sputtering yield is shown in figure 4 for 10 eVD^{-1} incident D_3^+ ions. As will be described in greater detail elsewhere [19], a systematic trend of the sputtering yields for the different molecular species compared at the same velocity has emerged from these comparative measurements: while

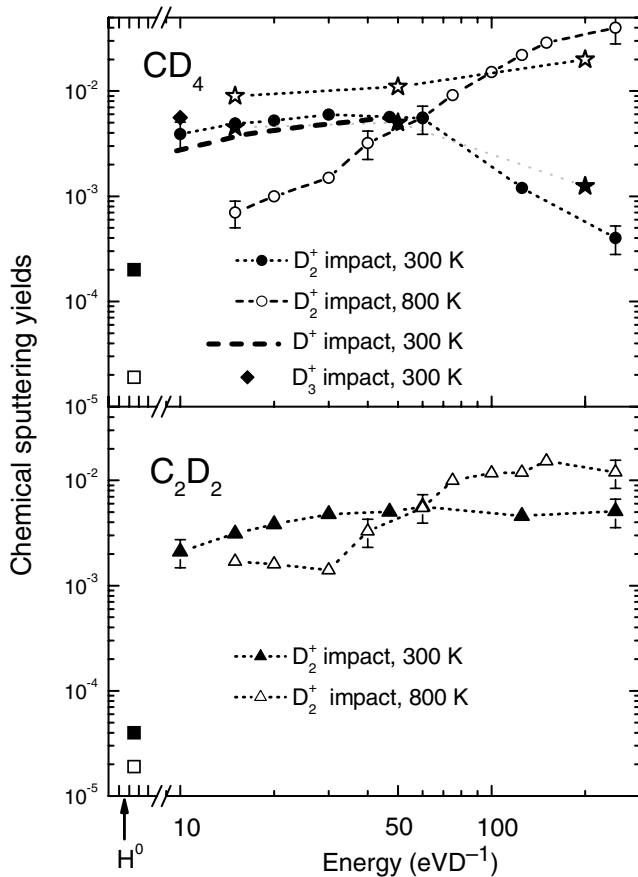


Figure 4. Chemical sputtering yield results for production of CD_4 and C_2D_2 . Open and solid circles, open and solid triangles, solid diamond and dashed line indicate present results; solid and open stars are results from [3] for 300 and 800 K sample temperatures, respectively; also shown are results from [7] for chemical erosion by thermal H atoms incident on pyrolytic graphite at 500 K (solid squares) and 800 K (open squares).

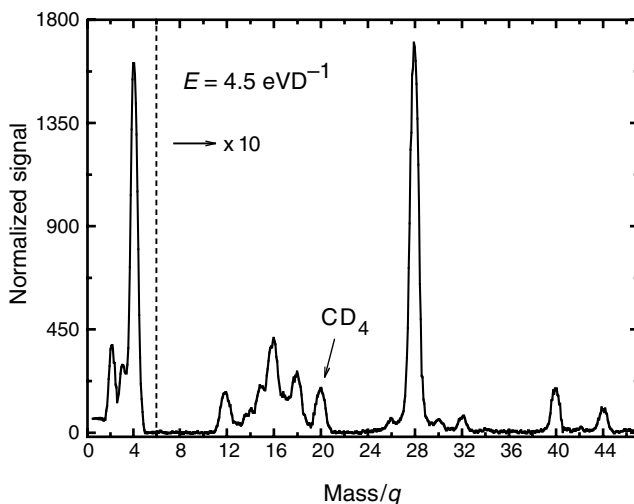


Figure 5. Background-subtracted mass spectrum for 4.5 eVD^{-1} D_3^+ incident ions, showing chemical sputtering production of CD_4 (mass 20).

all three species lead to chemical sputtering yields that agree within the experimental uncertainty at energies above about 60 eVD^{-1} , at lower energies the yields diverge by progressively larger amounts with decreasing energy, the incident triatomic molecular ion leading to the largest yields,

and atomic ion to the smallest. The difference at the lowest investigated energy amounts to more than a factor of two [19]. The reason for this divergence is not clear at present. At large incident energies, complete dissociation of the incident molecular species is very likely, and the fractional change of projectile kinetic energy due to dissociation energy release is relatively small. At the lowest impact energies, however, complete dissociation is no longer guaranteed. Moreover, if the dissociation occurs by electron capture before the ion enters the sample, significant broadening of the incident energy and angle is possible in the laboratory frame, due to the known amplification effects of the dissociation energy release (6–8 eV in this case) in the laboratory frame when the dissociation occurs in a moving frame. It would be interesting to investigate to what extent the experimentally observed differences can be accounted for by classical molecular dynamics simulations.

4. Discussion of mechanisms

For thermal energy H impact on a H-saturated graphite surface, the chemical erosion is essentially determined by the competition between H and CH_3 release [20]. Both processes are thermally activated. As a result there is little observed chemical erosion at room temperature for thermal energy impact. Since the activation energy of H release is slightly higher than that for CH_3 release, the chemical erosion reaches a maximum value with increasing sample temperature and then decreases back to zero.

For energetic H impact, hydrogenation and methyl group formation have been shown to occur at the end of the impacting ions' range in the graphite bulk, i.e., after thermalization of the incident ions [21, 22]. As a result, diffusion of methyl groups back to the surface plays an increasing role with increasing ion energy. Once the CH_3 reaction products reach the near-surface region, their kinetic ejection by non-thermalized incident particles augments the erosion resulting from thermally activated CH_3 release [21–24].

In this context, some of the general features of the present data are now qualitatively discussed. At the lowest investigated energies, the CD_4 production is very significant already for a room temperature sample, suggestive of the importance of the above-mentioned kinetic ejection mechanisms. Interestingly, at the lowest impact energies, the observed CD_4 production at 800 K is almost an order of magnitude lower than that observed at room temperature, indicative of the increased competition of the thermally activated D release noted above. As the ion impact energy is increased above 60 eVD^{-1} , the CD_4 yield decreases significantly at room temperature, suggesting decreased CD_3 survival during its diffusion back to the graphite surface. The methane yield for the 800 K sample temperature, on the other hand, increases strongly with increasing energy over the entire range investigated. One possibility for this dramatic increase could lie in the known strong increase of diffusion coefficients with temperature. A significantly reduced diffusion time of CD_3 back to the surface could increase their survival probability. In addition, the kinetic ejection itself may be

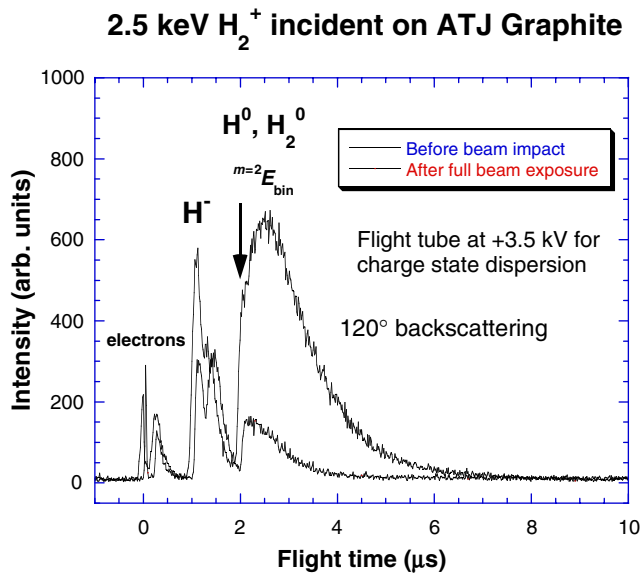


Figure 6. TOF spectrum for 2.5 keV H_2^+ incident on ATJ graphite, showing a significant component of H^- in the backscattered (dissociated) projectile spectrum; for two different beam exposure conditions: 'before beam impact' means sample exposure is limited to chopped (nanoampere intensity) H_2^+ beam; 'after beam exposure' means sample exposure of some minutes to full, unchopped (microampere intensity) H_2^+ beam. The label ' $m=2 E_{bin}$ ' in the figure designates the elastic binary collision energy for backscattering of a projectile with a mass of 2 amu from C at 120° .

slightly thermally activated, which would further enhance the production of free CD_4 .

In contrast, the energy dependences of the observed C_2D_2 yields are much weaker, as are the observed dependences on sample temperature. In light of the above discussion, the flatter energy dependence may suggest a reduced importance of diffusion processes for production of C_2D_2 , and thus may imply production more closely confined to the graphite near-surface region. A more detailed analysis of the temperature and energy dependence of the branching ratios for production of the different hydrocarbons, required to test this speculation, is beyond the scope of the present paper.

5. Planned TOF measurements

As has been alluded to already earlier, the partial pressure monitoring approach to chemical sputter yield determination suffers from having to determine wall corrections and from inability to measure production of radicals, i.e., the inability to determine the true product distribution of chemical sputtering species emerging from the graphite sample. For this reason, we plan in the near future to implement a TOF approach to complement the QMS measurements described above. Figure 1 illustrates schematically the TOF approach used in earlier measurements in our laboratory to study binary collision backscattering of multicharged ions from single crystal metal and alkali halide targets. This setup was used in preliminary studies of H backscattering from ATJ graphite at 2.5 keV, typical results for which are shown in figure 6. One feature of this TOF approach is the capability to analyse the charge state of backscattered projectiles by use of a floatable TOF drift tube, by differential acceleration of the

backscattered particles based on their charge, resulting in a dispersal in arrival times of the different charge states on the particle detector. The TOF system incorporates an electron impact ionizer at the entrance of the flight tube to facilitate the detection of neutrals at energies below their detection threshold on the multichannel plate, together with high-transmission biased grids before the ionizer to prevent unwanted entry of ions of either charge state into the TOF tube. The chopping scheme indicated in figure 1 used for the measurements of figure 6 will require modification for low-energy chemical sputter yield measurements, due to the likely loss of short-time correlation between the incident ion and the chemical sputtering product. One possible alternative that will be explored is the use of dual chopping: the first of the electron impact ionizer repeller grid to provide the required TOF mass resolution, and the second a slow chopping of the incident beam to permit accurate discrimination of events not directly related to the ion impact related chemical sputtering signal. By use of this technique, it is hoped that information on possible charge state distributions of the emitted chemical sputtering species, as well as their energy distributions, can be obtained. In addition, this approach should facilitate more detailed measurements on incidence angle dependences, which have not been available to date.

Acknowledgments

We are indebted to S H Overbury for making available the QMS and sample holder used in the present measurements. This research was sponsored by the Office of Fusion Energy Sciences and the Office of Basic Energy Sciences of the US Department of Energy under contract no DE-AC05-00OR22725 with UT-Battelle, LLC. LIV was appointed through the ORNL Postdoctoral Research Associates Program administered jointly by Oak Ridge Institute of Science and Education and Oak Ridge National Laboratory.

References

- [1] See e.g. Federici G this issue
- [2] Meyer F W 2000 *Trapping of Highly Charged Ions: Fundamentals and Applications* ed J Gillaspay (New York: Nova Science) pp 117–64
- [3] Wright G M, Haasz A A, Davis J W and Macaulay-Newcombe R G 2005 *J. Nucl. Mater.* **337** 74
- [4] Wright P B, Davis J W, Macaulay-Newcombe R G, Haasz A A and Hamilton C G 2001 *J. Nucl. Mater.* **290–293** 66
- [5] Mech B V, Haasz A A and Davis J W 1998 *J. Nucl. Mater.* **255** 153
Mech B V 1997 *PhD Thesis* Department of Aerospace Studies, University of Toronto, pp 52–55 unpublished
- [6] Mech B V, Haasz A A and Davis J W 1997 *J. Nucl. Mater.* **241–243** 1147
- [7] Davis J W, Haasz A A and Stangeby P C 1988 *J. Nucl. Mater.* **155–157** 234
- [8] Balden M and Roth J 2000 *J. Nucl. Mater.* **280** 39
- [9] Yamada R 1987 *J. Nucl. Mater.* **145–147** 359
- [10] Vietzke E, Flaskamp K, Phillips V, Esser G, Wienhold P and Winter J 1987 *J. Nucl. Mater.* **145–147** 443
- [11] Zecho T, Brandner B D, Biener J and Kupperts J 2001 *J. Phys. Chem. B* **105** 6194

- [12] Baloch M and Olander D R 1975 *J. Chem. Phys.* **63** 4772
- [13] Morozov V A and Meyer F W 1999 *Rev. Sci. Instrum.* **70** 4515
- [14] Meyer F W, Krause H F and Vergara L I 2005 *J. Nucl. Mater.* **337** 922
- [15] Morozov V A and Meyer F W 2001 *Phys. Rev. Lett.* **86** 736
- [16] Cornusca S, Diem A, Winter P, Aumayr F, Lorincik J and Sroubek Z 2002 *Nucl. Instrum. Methods B* **193** 616
- [17] Vergara L I, Meyer F W and Krause H F 2005 *J. Nucl. Mater.* submitted
- [18] See <http://vacuumtechnology.com/LEAKS/PSO.htm>
- [19] Vergara L I, Krause H F, Meyer F W and Nordlund K unpublished
- [20] Koppers J 1995 *Surf. Sci. Rep.* **22** 249
- [21] Roth J and Garcia-Rosales C 1996 *Nucl. Fusion* **36** 1647
- [22] Mech B V, Haasz A A and Davis J W 1998 *J. Appl. Phys.* **84** 16
- [23] Roth J and Bohdanský J 1987 *Appl. Phys. Lett.* **51** 964
- [24] Hopf C, von Keudell A and Jacob W 2002 *Nucl. Fusion* **42** L27